UDK 666.3:661.864.1
Original scientific article/Izvirni znanstveni članek

ISSN 1580-2949
MTAEC9, 58(3)413(2024)

DISPERSION OF AQUEOUS Y_2O_3 NANO-SUSPENSION AND FABRICATION OF TRANSPARENT CERAMICS BY COLLOIDAL PROCESSING

VODNA DISPERZIJA NANO DELCEV Y_2O_3 IN IZDELAVA PROSOJNE KERAMIKE S KOLOIDNIM POSTOPKOM

Jiao He*, Xin Zhang, Jingbao Lian, Xue Zhang, Mingxia Lei

School of Mechanical Engineering, Liaoning Petrochemical University, Fushun, 113001, P.R. China

Prejem rokopisa – received: 2024-03-05; sprejem za objavo – accepted for publication: 2024-04-22

doi:10.17222/mit.2024.1129

In the present study, transparent Y_2O_3 ceramics were successfully fabricated via colloidal processing, employing polyethylenimine (PEI) as an effective dispersant. The effect of PEI on nanosized Y_2O_3 suspensions was characterized by zeta-potential, adsorption behavior, rheological properties, and sedimentation test. The addition of PEI shifted the IEP of the Y_2O_3 powder towards a more alkaline pH range, and the adsorption of PEI on the Y_2O_3 surfaces gradually increased with the amount of PEI until reaching the saturation adsorption at 1.5 *w*/%. The PEI amount of 1.5 *w*/% was superior for the preparation of Y_2O_3 suspension as a result of a lower viscosity or sedimentation behavior. The viscosity of the suspension depended on the solids loading, increasing with the amount of powder. The optimal rheological behavior was achieved with 29 φ/% Y_2O_3 in the suspension, enabling the centrifugal slip casting of complex-shaped green bodies with a packing density of 43 %. Including an additional CIP treatment boosted the packing density of the green compacts, achieving above 50 %. Vacuum sintering the compacts at 1700 °C for 5 h yielded high-density ceramics exhibiting an in-line transmittance of approximately 73 % at a wavelength of 1100 nm.

Keywords: Y_2O_3, suspension, rheological behavior, transparent ceramics

V članku avtorji opisujejo uspešno izdelavo prosojne Y_2O_3 keramike s koloidnim postopkom. Pri tem so uporabili Polietilenimin (PEI) kot učinkovit dispergent. Učinek PEI na nanodelce Y_2O_3 v vodni suspenziji so določili z zeta potencialom, adsorpcijo, reološkimi lastnostmi in testom sedimentacije (posedanja), Dodatek PEI je premaknil izoelektrično točko (IEP) nano delcev Y_2O_3 bolj v smeri alkalnega pH območja in adsorpcija PEI na površinah nanodelcev Y_2O_3 je postopoma naraščala z vsebnostjo PEI dokler ni bilo doseženo adsorpcijsko nasičenje pri 1,5 *w*/%. Vsebnost PEI pri 1,5 *w*/% je bila optimalna za pripravo Y_2O_3 suspenzije, ker je le-ta imela majhno viskoznost in majhno nagnjenost k posedanju nano delcev. Viskoznost suspenzije je bila odvisna od deleža trdne faze oziroma je naraščala s povečevanjem deleža prašnih nano delcev. Optimalne reološke lastnosti so dosegli avtorji pri 29 φ/% Y_2O_3 v suspenziji. To je omogočilo postopek centrifugalnega nalivanja keramične gošče (angl.: centrifugal slip casting) kompleksnih oblik surovcev s 43 % gostoto pakiranja (nalivanja). Z dodatnim hladnim izostatskim stiskanjem (CIP; angl.: cold isostatic pressing) so gostoto surovcev povečali na približno 50 %. Sledilo je pet urno vakuumsko sintranje surovcev pri 1700 °C za tvorbo goste Y_2O_3 keramike. Transparentnost keramike so dosegli pri cca 73 % za valovno dolžino 1100 nm.

Ključne besede: Y_2O_3, suspenzija, reologija, transparentna keramika

1 INTRODUCTION

Transparent Y_2O_3 ceramics have aroused increasing research interest for many decades, primarily due to their excellent optical transparency over a wide wavelength range (0.2–8 μm), high thermal conductivity and low phonon energy, making them very suitable for various optical materials, such as IR windows and domes, host materials for solid-state laser or scintillator, and bulb envelopes, etc.[1–4] Widely accepted, achieving the fabrication of high-quality transparent ceramics requires special attention to each key step in ceramic production, namely, the synthesis of starting powders with excellent sintering activity, the consolidation of high-density and uniform green compacts, and the sintering of near-full-dense ceramics with pore-free structures.[5–7]

During the consolidation process, it is widely acknowledged that colloidal processing offers advantages in facilitating the production of large-sized and complex-shaped green compacts, exhibiting a homogeneous microstructure and the desired green density, whereas traditional dry uniaxial pressing methods often pose challenges in achieving such characteristics.[8–10] The critical technology of colloidal processing is to achieve a stable ceramic suspension with a high solids loading, low viscosity, and good dispersibility.[11,12] This is crucial for both enhancing the ease of handling and attaining a final product with high reliability. In both aqueous and non-aqueous nanopowder suspensions, the presence of a high surface area and a reduced separation distance among the nanoparticles gives rise to attractive interactions, thereby causing rapid settling and aggregation of the suspensions. Therefore, to get well-dispersed and stable nanopowder suspensions, the major stabilization

*Corresponding author's e-mail:
hejiao@lnpu.edu.cn (Jiao He)

mechanisms, including electrostatic, steric, or electrosteric stabilization mechanisms should be introduced in ceramic colloidal processing to offset the van der Waals attraction.[13] This often necessitates the addition of suitable dispersants that are adsorbed from solution onto the particle surfaces to control the interparticle forces, inhibit aggregation, and achieve stability.[14] Mouzon et al. found that electrosteric stabilization in the presence of polyelectrolyte A40 was effective for obtaining well-dispersed Y_2O_3 suspensions. The optimal concentration of A40 was determined to be 1.0 *w*/%, yielding the lowest viscosity of the suspension.[15] Sun prepared a stable suspension with 81 *w*/% solids loading, using water-soluble copolymer (0.2 *w*/% Ib104 plus 0.3 *w*/% Ib600) as both a dispersing and gelling agent.[16] The transmittance measured at 1100 nm of the resultant Y_2O_3 ceramics was found to be 80.9 %. More recently, a novel aqueous colloidal processing route has been explored to improve the stability and dispersion of Y_2O_3 suspensions through the combined use of a ZrO_2 coating agent and polyelectrolyte dispersant.[17] However, the use of the coating agent necessitates a higher sintering temperature or pressure-assisted sintering during the sintering process in order to densify the final products. Over the past few decades, a series of anionic polymers has often been utilized to effectively improve the stability of Y_2O_3 suspensions.[18–20] However, fewer investigations of the preparation of Y_2O_3 aqueous suspension by adding cationic dispersants have been reported, and those available were not systematic.

Polyethylenimine (PEI) has been employed as a cationic dispersant to enhance the stability of various ceramic powder suspensions such as ZrO_2,[21] Y-TZP,[22] SiC,[23] and Si_3N_4.[24] In a neutral or acidic environment, the positively charged PEI could adsorb on ceramic particle surfaces, resulting in an electrosteric effect that hinders the flocculation of the ceramic suspension.[21] Xu et al. reported that PEI was used as a dispersant to improve the dispersion properties of Y_2O_3 powders (average particle size of 200 nm) in ethanol. Adding 1.5 *w*/% PEI, a Y_2O_3 alcoholic suspension with a solids loading of 20.8 φ/% and a viscosity of less than 0.1 Pa·s at a shear rate of 10 s^{-1} was obtained.[25] In this work, PEI was selected as a dispersant for aqueous Y_2O_3 suspensions. The colloidal properties of Y_2O_3 suspensions with regard to PEI amount are extensively elucidated. In addition, the effect of ceramic solids loading on the rheological properties of the PEI-based suspensions was also explored. Subsequently, the optimal conditions for Y_2O_3 suspensions were determined and used to produce cylindrical green compacts by centrifugal slip casting. Then the vacuum sintering was carried out to fabricate the Y_2O_3 ceramics. Finally, optical transmission of the resultant sintered samples was examined.

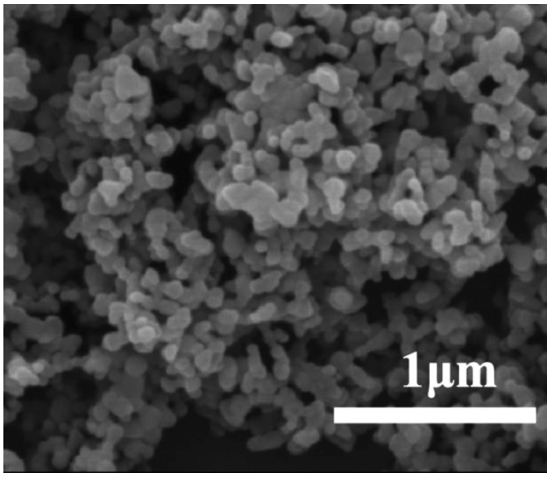

Figure 1: SEM micrograph of the Y_2O_3 powder

2 EXPERIMENTAL PART

2.1. Raw materials

In the present study, commercially available, high-purity Y_2O_3 (99.99%) was utilized. This powder has a specific surface area of 8.17 m^2/g measured through N_2 adsorption (Model TriStar II 3020, Micrometritics Instrument Corp., Norcross, GA) The morphology of the as-received powder, measured by scanning electron microscopy (SEM), is illustrated in **Figure 1**, revealing that the primary particle size was approximately 96 nm. Before preparing the suspension, the powder underwent pretreatment. Polyethyleneimine (PEI) (Sinopharm Chemical Reagent Co., Ltd., Shanghai, China), with an average molecular weight of 10,000 was taken as the dispersant.

2.2 Preparation process

A series of Y_2O_3 suspensions at a solids loading of 5 φ/%, containing increasing amounts of dispersant (expressed as the total mass of Y_2O_3 powder), were prepared. In a typical procedure, the dispersant was dissolved in distilled water in a polyethylene jar containing zirconia balls. Then Y_2O_3 powder was gradually added to the mixture. The resultant suspensions were ball-milled for 6 h in a planetary mill.

Various suspensions at the optimal dispersant amount with a solids loading ranging from 10 φ/% to 31 φ/% for different ball-milling times were prepared following the same procedure.

Y_2O_3 green bodies were fabricated by a centrifugal slip-casting method. Selected, concentrated Y_2O_3 suspensions were poured into the molds and left for consolidation using a laboratory centrifuge at constant speed of 3000 min^{-1} for 40 min. After 24 h at room temperature, the green bodies were extracted from the mold, and further oven dried at 80 °C for over 12 h. Then, the green bodies were pre-sintered at 1000 °C for 4 h in a muffle furnace to remove the organic additives, and subsequently sintered at 1700 °C for 5 h in a vacuum of

1.0×10^{-3} Pa in a furnace with a molybdenum heating element (VSF-7, Shenyang, China).

2.3 Characterization and test

The zeta-potential of the aqueous Y_2O_3 suspension was estimated by an acoustic and electroacoustic spectrometer (DT-1202, Dispersion Technology Inc., Bedford Hills, USA). In this measurement, 5 *w*/% Y_2O_3 suspension was employed and the pH was adjusted using 1 mol/L HCl and 1 mol/L KOH aqueous solution.

To study the adsorption behavior of the PEI, Y_2O_3 suspensions with 5 φ/% solids loading were utilized. The as-received suspensions were centrifuged at 3000 min^{-1} for 40 min, the supernatants were poured out and the sediments were dried in the oven at 100 °C for 5 h. Afterwards, the adsorbed amount of PEI was determined using a DTA/TG analyzer (Model SETSYS Evolution-16, Setaram, Lyons, France) by measuring the weight loss of the dried powders during heating in a flowing oxygen atmosphere.

Rheological behavior mainly focuses on the viscosity curve of Y_2O_3 suspensions that were evaluated using a cone-plate viscometer (Brookfield DV-II+Pro, Brookfield Engineering Laboratories, USA) at room temperature.

The stability of the Y_2O_3 suspension was easily characterized by sedimentation tests, which offer an approximation of colloidal stability. The suspensions were kept in glass graduated cylinders for more than 60 h and the volume of the sedimentation as a percentage of the total suspension volume (Normalized volume) was measured as a function of settling time.

Archimedes' immersion method was applied to determine the densities of the obtained green bodies. The relative density was determined by calculating the ratio of the actual density to the theoretical density of Y_2O_3, using distilled water as the immersion medium. The microstructure of the green bodies was observed using a field-emission scanning electron microscope (FE-SEM). The samples were cut into fractured slices, and subsequently coated with gold to enhance their conductivity before being examined. Subsequently, polished pellets with a thickness of 1.2 mm, which were cut from the sintered specimens, were employed to measure the optical transmittance using an ultraviolet/visible/near-infrared spectrophotometer (Model Lambda 750S, Perkin Elmer, CT, USA).

3 RESULTS AND DISCUSSION

3.1 Optimization of PEI amount

As previously mentioned, achieving effective colloidal processing and maximizing uniformity in the green bodies depends on the ability to produce a suspension that is not only well-dispersed, but also possesses a relatively high solids loading.[26] This objective was realized through the addition of the PEI dispersant to a water-based solution, effectively stabilizing the suspension. The optimization of the operational parameters was identified through a sequence of analyses and assessments.

Zeta-Potential Analysis **Figure 2** illustrates the relationship between the zeta-potential value and the amount of PEI for individual fresh dilute suspensions of Y_2O_3. For Y_2O_3 powder without PEI, increasing the pH value from 6.2 to a significantly basic range, the surface charges of the particles experienced a notable shift, transitioning from a positive charge to a negative charge. This shift was a clear sign of an isoelectric point (IEP) of approximately 9.7, where the suspension was in its least stable state in terms of particle agglomeration. With the increasing of the pH, a steep increase is observed in the absolute value of the zeta potential. In the case of Y_2O_3 containing 0.5 *w*/% PEI, the values of the zeta potential changed to positive across the pH range < 10.9, indicating PEI successfully adsorbed on the surface of Y_2O_3 particles. This phenomenon can be attributed to the fact of polyethyleneimine (PEI) being a cationic polyelectrolyte. When acid was introduced to a suspension containing PEI, it reacted with the basic –NH– groups in PEI, leading to their neutralization and the formation of a positively charged polymer structure ($–NH^{2+}–$).[23] Consequently, these positively charged groups exhibited a strong affinity for adsorption onto negatively charged Y_2O_3 surfaces through electrostatic interactions, causing a shift in the IEP towards a more alkaline range. Then, at a higher PEI amount of 1.5 *w*/%, the IEP moved to a pH of 11 due to the absorption of PEI on the Y_2O_3 particles. With the further increasing amount of PEI, there was no notable alteration in the zeta-potential, indicating a state of saturation adsorption. Additionally, both within the selected amount range of PEI and across the entire pH range, the absolute value of the potential remained below 30 mV, indicating a lack of sufficient electrostatic repulsion to disperse the powder particles.

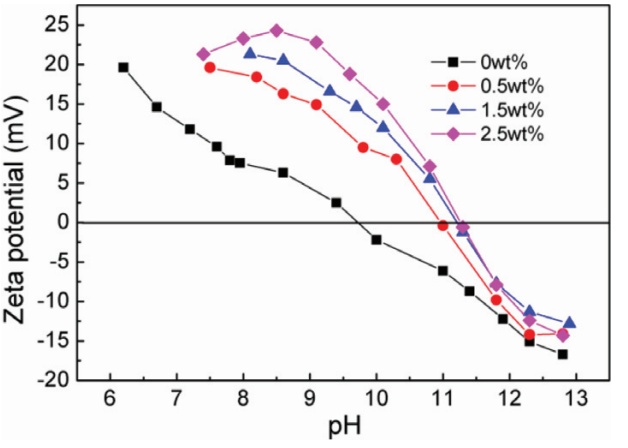

Figure 2: Zeta-potential of Y_2O_3 particles in the absence and presence of various amounts of PEI

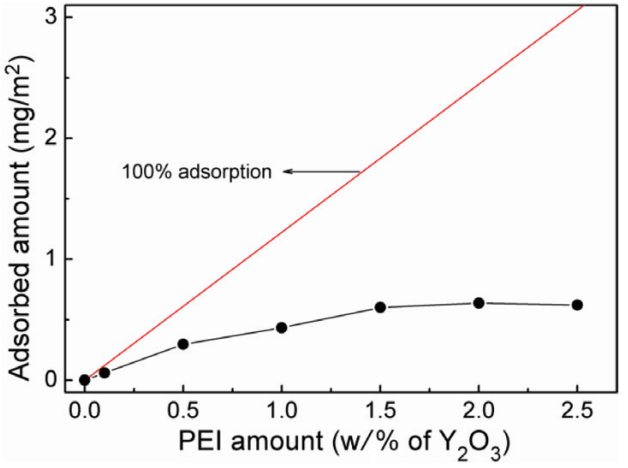

Figure 3: Adsorption amount of PEI in Y_2O_3 suspensions versus the amount of added PEI

Adsorption of PEI onto Y_2O_3 particles

Figure 3 presents the variation in the adsorption amount of PEI on the surface of Y_2O_3 powder particles as a function of the initial PEI addition. As evident from **Figure 3**, the adsorption of PEI on the surface of Y_2O_3 particles gradually rose with an increase in PEI amount from 0.1 *w*/% to 1.5 *w*/%. Afterwards, a saturation adsorption amount of 0.5 mg/m^2 was observed. The adsorption amount was kept almost constant as the PEI amount exceeded 1.5 *w*/%, revealing that PEI on the surface of Y_2O_3 particles had reached its adsorption limit, in agreement with the results of the zeta-potential measurement.

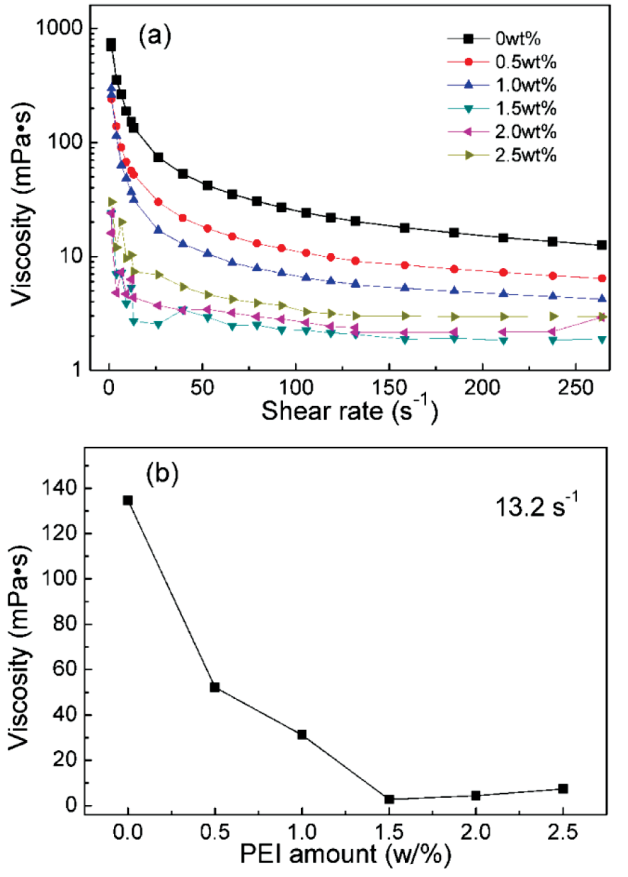

Figure 4: Evolution of the viscosity of Y_2O_3 suspensions as a function of PEI amount

Suspension Rheological Properties

Dispersants play a role in improving the rheological and dispersion stability of suspensions, both of which are very dosage-sensitive. **Figure 4** depicts the variations in the viscosity of the Y_2O_3 suspensions with varying PEI amounts in the range from 0 *w*/% to 2.5 *w*/%, at the shear rate of 1.32–264 s^{-1}. All Y_2O_3 suspensions exhibited clear shear thinning behavior, indicative of a non-Newtonian rheological behavior. As is obvious in **Figure 4a**, the inclusion of PEI dispersant notably enhanced the stability of the Y_2O_3 suspension, exhibiting a rapid reduction in viscosity as the increased PEI amount in the range of not exceeding 1.5 *w*/%, as a result of the absorption of PEI on the surfaces of powder particles. Upon regulating the PEI amount from 0 *w*/% to 1.5 *w*/%, the viscosity of Y_2O_3 suspensions presented a substantial transformation, shifting from 134.7 mPa·s to 2.7 mPa·s at a shear rate of 13.2 s^{-1}, as seen in **Figure 4b**. Then, at higher PEI contents of up to 2.0 *w*/% and 2.5 *w*/%, a minor increase in the viscosity of the suspension was detected. This observation was explained by the mutual cross-linking effect of the PEI after reaching adsorption saturation on the powder surfaces, which subsequently led to a deterioration in the stability of the suspension. The suspension containing 1.5 *w*/% PEI exhibited the lowest viscosity value, which is indicative of a superior suspension stability, enabling easy particle movement.

Sedimentation test

A sedimentation plot versus the time of Y_2O_3 suspensions with various PEI amounts is presented in **Figure 5**. It is observed from **Figure 5** that the suspension in the absence of PEI settled rapidly within 30 min. After 120 min, the normalized volume of the suspensions at-

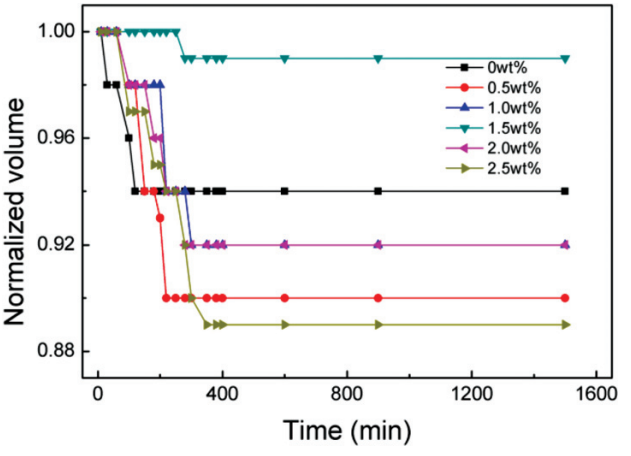

Figure 5: Variation of sedimentation volume versus time of Y_2O_3 suspensions with various amounts of PEI

tained a value of 0.94. Further extending the settling time, it was noted that the sedimentation volume of the suspension remained unchanging, indicating the occurrence of severe flocculation. Y_2O_3 nanoparticles with a high surface energy easily gave rise to severe agglomeration among the particles. This agglomeration, in turn, triggered flocculation within the suspension, ultimately leading to the complete loss of fluidity among the particles in the suspension. In the case of containing PEI, the starting settling time of the slurry was delayed, and settling was observed to be much slower, due to the PEI adsorbed on the Y_2O_3 powder. PEI is a highly branched macromolecule with a general chemical formula of $[–CH_2–CH_2–NH–]_n$.[23] The partially ionized or non-ionized PEI could adsorb onto the negatively charged surface and thus provide an electrosteric or steric stabilization for ceramic suspensions. It was reported that the degree of PEI dissociation (α) exhibits an increasing trend as the pH decreases, and partially dissociated PEI with $\alpha = 0.1$ at pH≈10 can be obtained.[24] The pH of the suspension without pH adjustment was approximately 9.4, at which α value of partially dissociated PEI was ≈0.1. In all cases of suspensions with PEI, the low absolute potential indicated that positively charged polymer groups adsorbed onto the surface of powder could not provide sufficient electrostatic repulsive force to prevent the aggregation of particles, As seen from the results of the zeta-potential measurement in **Figure 2**. Moreover, lower viscosity and sedimentation of suspensions with PEI were achieved, revealing that the stabilization of suspensions may be dominated by incorporation of electrosteric and steric effects developed from the ionized and unionized PEI. The higher sedimentation can be explained in view of the lack of enough electrosteric or steric forces to overcome the Van der Waals attraction force for PEI amounts less than 1.0 *w*/%, due to incomplete coverage of the Y_2O_3 particle surfaces. However, after a certain amount of 1.5 *w*/%, the settling volume increased again due to excessive PEI molecules in solution. A mass of free polymers in solution entangled with each other, thus causing depletion flocculation.[22] The optimum PEI amount that can be added to a Y_2O_3 suspension to achieve suspension stability was found to be 1.5 *w*/%, which possessed the lowest viscosity and small sedimentation.

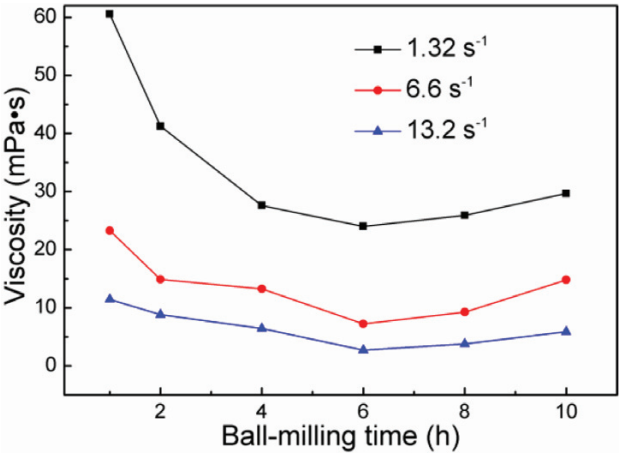

Figure 6: Variation of viscosity for Y_2O_3 suspensions as a function of ball-milling times

Optimization of dispersion time

The viscosity presented in **Figure 6** shows the efficiency of ball-milling time on the stability of suspensions containing 1.5 *w*/% PEI, as a function of shear rate. It is evident that as the ball-milling time increased, the viscosity of the suspension decreased significantly. At a ball milling time of 1 h, the viscosity measured at a shear rate of 1.32 s^{-1} was 60.55 mPa·s. Moreover, upon reaching a ball-milling time of 6 h, the viscosity attained its minimal value of ≈24 mPa·s at 1.32 s^{-1}, which indicated the finest homogeneity in the Y_2O_3 system. Further extending the ball milling time to 8 h and 10 h resulted in a slight increase in viscosity to 25.90 mPa·s and 29.66 mPa·s, respectively. The purpose of ball milling is to achieve a uniformly dispersed suspension through the collisions between the milling balls and Y_2O_3 particles. In the initial stages of ball milling, specifically at 1 h and 2 h, the process focused on refining and homogenizing the powder particles. The application of external force through ball milling could enhance the penetration of the dispersing medium, resulting in its uniform dispersion among the Y_2O_3 particles. Additionally, this refined process effectively eliminated particle agglomeration and promoted the uniform adsorption of PEI onto the Y_2O_3 powder surfaces. Thus, increasing the ball-milling time could enhance the stability and fluidity of the Y_2O_3 suspensions, manifesting as a decrease in viscosity. However, the powder particles may become excessively grinded and refined under prolonged mechanical impact of 8 h or 10 h, causing the higher specific surface area. These increases made the decrease in available volume of the dispersing medium within the system, narrowing the distance between the particles. Consequently, the Van der Waals attractive force increased and favored particle agglomeration, leading to an elevation in suspension viscosity and a subsequent decline in ball-milling efficiency. Furthermore, the higher specific surface area of the Y_2O_3 particles indicated that more of their surfaces were exposed into the liquid phase, causing the 1.5 *w*/% PEI dosage to give inadequate coverage of the Y_2O_3 particle surfaces. Besides, a prolonged dispersion time can induce severe hydrolysis behavior of the nanosized Y_2O_3 powders and cause a significant amount of trivalent yttria cations and their hydroxo complexes in the suspension, strongly decreasing the stability of the suspension, shown by the following equations :[27]

$$OH^- + {}^+H_2O - Y = Y - OH + H_2O = \\ = Y - O^- + H_30^+ \quad (1)$$

$$Y^{3+} + 3OH^- = Y(OH)_3\ (s) \quad (2)$$

$$Y^{3+} + OH^- = Y(OH)^{2+} \quad (3)$$

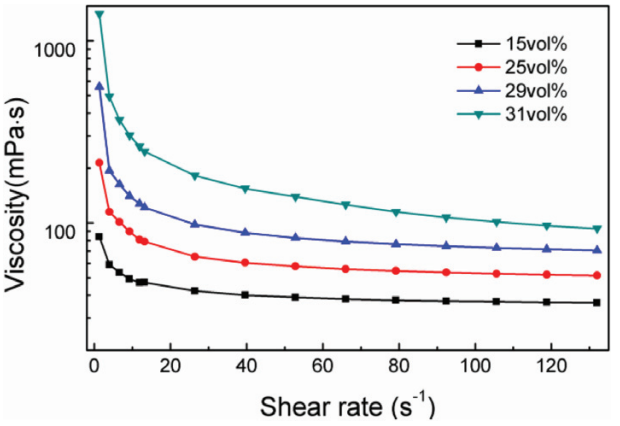

Figure 7: Effect of different solids loading on the rheological property of Y_2O_3 suspensions containing 1.5 *w*/% PEI

$$2Y^{3+} + 2OH^- = Y_2(OH)_2^{4+} \quad (4)$$

Therefore, in this experiment, ball milling for 6 h was determined as the optimum dispersion condition.

Rheological study to optimize solids loadings of Y_2O_3 suspension

In colloidal processing, carefully controlling the appropriate solids loading of the suspension is crucial for achieving optimal particle packing in the green body, while also maintaining a suitable viscosity. Viscosity measurements were conducted at varying shear rates to investigate the impact of solids loading on the rheological behavior, as depicted in **Figure 7**. The solids loading of Y_2O_3 was varied from 15 φ/% to 31 φ/%. From **Figure 7**, it is observed that all the suspensions showed shear thinning behavior. Under the tested range of shear rates, the suspension containing 15 φ/% solids loading exhibited lower viscosity than the other suspensions. This suspension exhibiting a remarkably low viscosity demonstrated exceptional fluidity, yet it was insufficiently viscous to form perfect green bodies. Therefore, it is advisable to elevate the solids loading to attain green bodies with a higher density. As **Figure 7** shows, the viscosity of the suspension substantially boosted by increasing the solids loading. In all the cases, the viscosity of the suspension changed from 84.0 mPa·s to 1401.8 mPa·s at a shear rate of 1.32 s^{-1}. when the solids loading exceeded 31 φ/%, it became too stiff to meet the testing-range requirements. This is attributed to the fact of higher hydrodynamic interaction resulting from the increasing number of particles as the solids loading increased. Additionally, by elevating the solids loading, the mean distance between the particles decreased, as a result, an intensified attractive force among them, leading to an increased viscosity. In the case of 29 φ/%, the suspension exhibited a viscosity of less than 1000 mPa·s over a broad range of shear rates. This level of solids loading proved advantageous not only for achieving a high density of green bodies but also for casting.

Consolidation of Y_2O_3 suspensions and sintering of transparent ceramics

Consolidation of the green bodies using suspensions with various solids loading and 1.0 *w*/% PEI added was performed by centrifugal slip casting. **Figure 8** demonstrates the influence of solids loading on the green relative density. As evident from **Figure 8**, the sample with a solids loading of 29 φ/% exhibited the highest packing density of ≈43%. As the solids loading increased, the green relative density also increased. However, an exception was observed for the sample with 31 φ/%, which exhibited a slightly lower density than the sample with 29 φ/%. This deviation can be attributed to unsuitable rheological properties of the suspension, which aligned with the rheological behavior in **Figure 7**.

Figure 9 shows the fracture surfaces of Y_2O_3 green bodies with different solids loadings. There was a difference in the homogeneity among these samples. The green compacts for 15 φ/% showed a poor dispersion of particles due to excessively low solids loading. At a 29 φ/% solids loading, a more homogeneous and compact microstructure with small open pores can be observed. In sharp contrast, serious agglomeration and large pores were discovered in the green bodies of 31 φ/% suspension, thereby decreasing their density and homogeneity.[28] It is well known that green compacts exhibiting a narrow open pore size distribution and a uniform microstructure demonstrate superior sinterability, enabling facile densification at relatively lower sintering temperatures. According to the above analysis, the green bodies, which contained 1.5 *w*/% PEI and possessed a solids loading of 29 φ/%, were selected for the fabrication of transparent ceramics. However, the packing density of 43 % achieved was inadequate for subsequent pressureless sintering due to their porous structure. To further boost the packing density of the consolidated green bodies, an additional CIP treatment was utilized at a pressure of 200 MPa. The obtained green bodies demonstrated exceptional compressibility. Following the CIP treatment, the densities of the samples increased to over

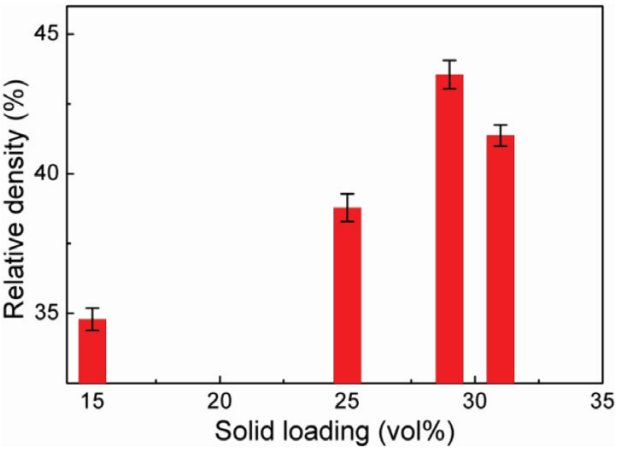

Figure 8: Relative density of cast green bodies from various solids loading suspensions

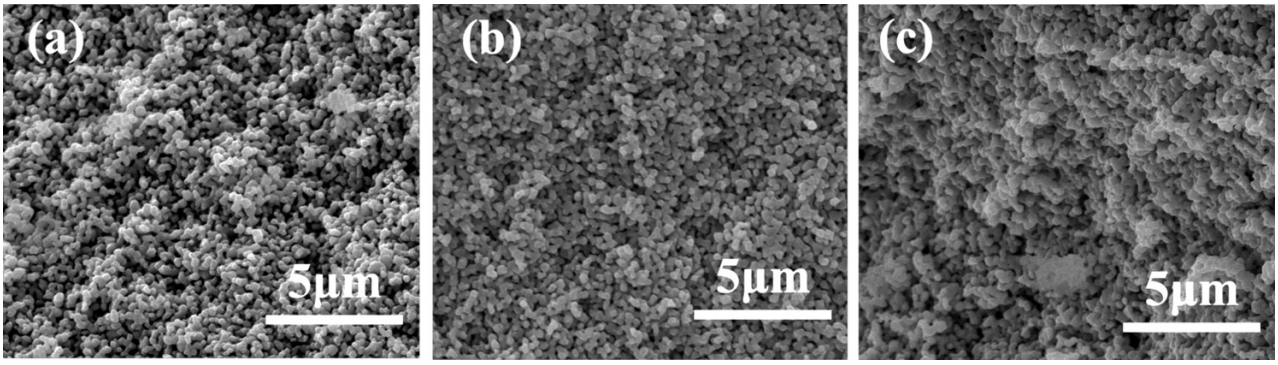

Figure 9: SEM micrographs of the fracture surfaces of the green bodies obtained from the suspension with various solids loading: a) 25 φ/%, b) 29 φ/%, c) 31 φ/%

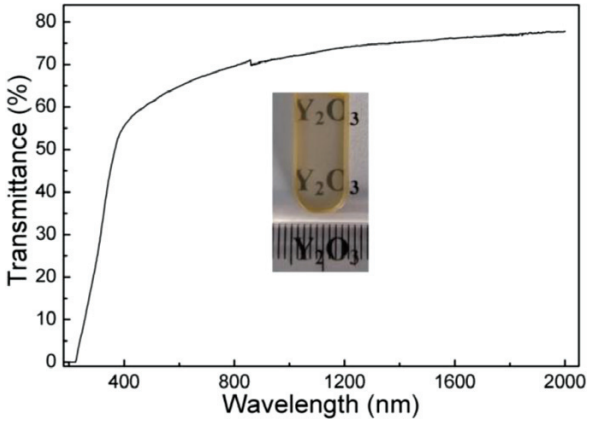

Figure 10: In-linear transmittance of 1.2-mm-thick Y_2O_3 ceramic. Inset showing an image of polished Y_2O_3 ceramics

50 %, indicating a significant improvement in their compaction properties.

Vacuum sintering was carried out on the consolidated green bodies. The relative density of the centrifugally cast ceramics was ≈99.9 %. **Figure 10** shows the optical transmission spectra of the mirror-polished Y_2O_3 ceramic specimen with a thickness of 1.2 mm. At the wavelengths of 1100 nm and 2000 nm, the in-line transparency approached 73 % and 78 %, respectively. The inset in **Figure 10** is the corresponding image of the as-obtained ceramic specimen, exhibiting an approximate diameter of 9 mm and a length extending to 20 mm. Notably, the letters below the ceramic specimen were clearly visible, further emphasizing their remarkable optical transparency.

4 CONCLUSIONS

Transparent Y_2O_3 ceramics were prepared using a colloidal processing technique, employing nano-sized Y_2O_3 powders as the starting material. The effectiveness of the PEI in enhancing the colloidal stability of the aqueous Y_2O_3 suspension was investigated. The introduction of PEI shifted the IEP of Y_2O_3 powder towards a higher pH value. The adsorption of PEI on the Y_2O_3 surface increased with the amount of PEI and reached saturation adsorption at 1.5 *w*/%. A well-dispersed Y_2O_3 suspension was obtained at an amount of 1.5 *w*/%, at which the viscosity and sedimentation volume of the suspension decreased to a minimum value. By optimizing the ball-milling time, the stability of the suspension can be significantly improved. The viscosity of the suspension exhibited a dependence on solids loading, demonstrating an increase as the amount of powder boosted. A higher solids loading with suitable rheological behavior was achieved in the case of 29 φ/% of Y_2O_3 in the suspension, which for centrifugal slip casting led to complex-shaped green bodies with a packing density of 43 %. By incorporating an additional CIP treatment, the packing density of the green compacts can be elevated beyond 50 %. Subsequently, vacuum sintering at 1700 °C for 5 h resulted in high-density ceramics with an in-line transmittance of approximately 73 % at 1100 nm.

Acknowledgments

This work was supported by the National Natural Science Foundation of China (Grant No. 51802136), Foundation of Liaoning Educational Committee (Grant No. L2020043).

5 REFERENCES

[1] H. M. Oh, Y. J. Park, H. N. Kim, J. W. Ko, H. K. Lee, Effect of milling ball size on the densification and optical properties of transparent Y_2O_3 ceramics, Ceram. Int., 47 (**2021**) 4, 4681–4687, doi:10.1016/j.ceramint.2020.10.035

[2] D. Permin, O. Postnikova, S. Balabanov, A. Belyaev, V. Koshkin, O. Timofeev, J. Li, Influence of SHS precursor composition on the properties of yttria powders and optical ceramics, Materials., 16 (**2023**) 1, 260, doi:10.3390/ma16010260

[3] A. Ratsimba, A. Zerrouki, N. Tessier-Doyen, B. Nait-Ali, D. André, P. Duport, A. Neveu, N. Tripathi, F. Francqu, G. Delaizir, Densification behaviour and three-dimensional printing of Y_2O_3 ceramic powder by selective laser sintering, Ceram. Int., 47 (**2021**) 6, 7465–7474, doi:10.1016/j.ceramint.2020.11.087

[4] L. Gan, Y. J. Park, M. J. Park, H. Kim, J. M. Kim, J. W. Ko, J. W. Lee, Facile fabrication of highly transparent yttria ceramics with fine microstructures by a hot-pressing method, J. Am. Ceram. Soc., 98 (**2015**) 7, 2002–2004, doi:10.1111/jace.13648

[5] X. R. Zhang, W. Z. Lu, G. F. Fan, X. H. Wang, Fabrication of well-dispersed Y_2O_3 nano-powders by poly (acrylic acid) low-temperature combustion, Adv. Powder Technol., 27 (**2016**) 1, 295–298, doi:10.1016/j.apt.2015.11.004

[6] F. F. Lange, Powder processing science and technology for increased reliability, J. Am. Ceram. Soc., 72 (**1989**) 1, 3–15, doi:10.1111/j.1151-2916.1989.tb05945.x

[7] L. L. Zhu, Y. J. Park, L. Gan, S. I. Go, H. N. Kim, J. M. Kim, J. W. Ko, Effects of the Zr concentration on transparent Y_2O_3 Ceramics fabricated by vacuum pre-sintering and a subsequent HIP treatment, J. Mater. Sci. Mater. Electron., 28 (**2017**), 7854–7861, doi:10.1007/s10854-017-6482-9

[8] J. A. Lewis, Colloidal processing of ceramics, J. Am. Ceram. Soc., 83 (**2000**) 10, 2341–2359, doi:10.1111/j.1151-2916.2000.tb01560.x

[9] X. Y. Zhang, W. L. Huo, S. Yan, Y. G. Chen, K. Gan, J. J. Liu, J. L. Yang, Innovative application of PVA hydrogel for the forming of porous Si_3N_4 ceramics via freeze-thaw technique, Ceram. Int., 44 (**2018**) 11, 13409–13413, doi:10.1016/j.ceramint.2018.03.071

[10] A. Shafeiey, M. H. Enayati, A. Al-Haji, The effect of slip casting parameters on the green density of $MgAl_2O_4$ spinel, Ceram. Int., 43 (**2017**) 8, 6069–6074, doi:10.1016/j.ceramint.2017.01.151

[11] F. Mohammadi, O. Mirzaee, M. Tajally, Influence of solids loading on the rheological, porosity distribution, optical and the microstructural properties of YAG transparent ceramic, Ceram. Int., 44 (**2018**) 11, 12098–12105, doi:10.1016/j.ceramint.2018.03.230

[12] V. M. Candelario, M. I. Nieto, F. Guiberteau, R. Moreno, A. L. Ortiz, Aqueous colloidal processing of SiC with $Y_3Al_5O_{12}$ liquid-phase sintering additives, J. Eur. Ceram. Soc., 33 (**2013**) 10, 1685–1694, doi:10.1016/j.jeurceramsoc.2013.01.030

[13] G. V. Franks, C. Tallon, A. R. Studart, M. L. Sesso, S. Leo, Colloidal processing: enabling complex shaped ceramics with unique multiscale structures, J. Am. Ceram. Soc., 100 (**2017**) 2, 458–490, doi:10.1111/jace.14705

[14] I. Santacruz, M. J. Zayas-Rey, J. M. Porras-Vázquez, D. Marrero-López, E. R. Losilla, Colloidal processing and characterisation of lanthanum tungstate sheets, $La_{5.5}WO_{11.25}$, prepared by tape casting and reaction sintering, Ceram. Int., 41 (**2015**) 9, 11334–11340, doi:10.1016/j.ceramint.2015.05.091

[15] J. Mouzon, E. Glowacki, M. Oden, Comparison between slip-casting and uniaxial pressing for the fabrication of translucent yttria ceramics, J. Mater. Sci., 43 (**2008**) 2849–2856, doi:10.1007/s10853-007-2261-y

[16] Y. Sun, S. Z. Shimai, X. Peng, G. H. Zhoua, H. Kamiyac, S. W. Wang, Fabrication of transparent Y_2O_3 ceramics via aqueous gelcasting, Ceram. Int., 40 (**2014**) 6, 8841–8845, doi:10.1016/j.ceramint.2014.01.106

[17] Z. C. Fu, X. D, Li, Y. Ren, M. Zhang, X. T. Geng, Q. Zhu, J. G. Li, X. D. Sun, Coating Y_2O_3 nano-particles with ZrO_2-additive via precipitation method for colloidal processing of highly transparent Y_2O_3 ceramics, J. Eur. Ceram. Soc., 39 (**2019**) 15, 4996–5004, doi:10.1016/ j.jeurceramsoc.2019.07.011

[18] G. B. Granger, C. Guizard, Sintering behavior and optical properties of yttria, J. Am. Ceram. Soc., 90 (**2007**) 9, 2698–2702, doi:10.1111/j.1551-2916.2007.01759.x

[19] L. L. Jin, X. J. Mao, S. W. Wang, M. J. Dong, Optimization of the rheological properties of yttria suspensions, Ceram. Int., 35 (**2009**) 2, 925–927, doi:10.1016/j.ceramint.2008.03.009

[20] J. He, X. D. Li, Q. Zhu, C. Ma, M. Zhang, J. G. Li, X. Sun, Dispersion of nano-sized yttria powder using triammonium citrate dispersant for the fabrication of transparent ceramics, Ceram. Int., 42 (**2016**) 8, 9737–9743, doi:10.1016/j.ceramint.2016.03.064

[21] C. Duran, Y. Jia, Y. J. Hotta, K. Sato, K. Watari, Colloidal processing, surface characterization, and sintering of nano ZrO_2 powders, J. Mater. Res., 20 (**2005**), 1348–1355, doi:10.1557/JMR.2005.0168

[22] C. H. Chin, A. Muchta, C. H. Azhari, M. Razali, M. Aboras, Optimization of pH and dispersant amount of Y-TZP suspension for colloidal stability. Ceram. Int., 41 (**2015**) 8, 9939-9946, doi:10.1016/j.ceramint.2015.04.073

[23] J. Sun, L. Gao, Dispersing SiC powder and improving its rheological behavior, J. Eur. Ceram. Soc., 21 (**2001**) 13, 2447–2451, doi:10.1016/S0955-2219(01)00196-0

[24] X. W. Zhu, T. Uchikoshi, T. S. Suzuki, Y. Sakka, Effect of Polyethylenimine on Hydrolysis and Dispersion Properties of Aqueous Si_3N_4 Suspensions, J. Am. Ceram. Soc., 90 (**2007**) 3, 797–804, doi:10.1111/j.1551-2916.2007.01491.x

[25] Y. Y. Xu, X. J. Mao, J. T. Fan, X. K. Li, M. H. Feng, B. X. Jiang, F. Lei, L. Zhang, Fabrication of transparent yttria ceramics by alcoholic slip-casting, Ceram. Int., 43 (**2017**) 12, 8839–8844, doi:10.1016/j.ceramint.2017.04.017

[26] D. Marani, B. R. Sudireddy, J. J. Bentzen, P. S.Jørgensen, R. Kiebach, Colloidal stabilization of cerium-gadolinium oxide (CGO) suspensions via rheology, J. Eur. Ceram. Soc., 35 (**2015**) 10, 2823–2832, doi:10.1016/j.jeurceramsoc.2015.03.043

[27] Z. Q. Sun, X. W. Zhu, M. S. Li, Y. C. Zhou, Y. Sakka, Hydrolysis and dispersion properties of aqueous $Y_2Si_2O_7$ suspensions, J. Am. Ceram. Soc., 92 (**2009**) 1, 54–61, doi:10.1111/j.1551-2916.2008.02860.x

[28] A. Goswami, K. Ankit, N. Balashanmugam, A.M. Umarji, G. Madras, Optimization of rheological properties of photopolymerizable alumina suspensions for ceramic microstereolithography, Ceram. Int., 40 (**2014**) 2, 3655–3665, doi:10.1016/j.ceramint.2013.09.059